Bioorganic & Medicinal Chemistry 28 (2020) 115731

Contents lists available at ScienceDirect

Bioorganic & Medicinal Chemistry

journal homepage: www.elsevier.com/locate/bmc

Fragment based drug design and diversity-oriented synthesis of carboxylic acid isosteres

Martina Ferri[a,1], Manuel Alunno[a,1], Francesco Antonio Greco[b], Andrea Mammoli[a], Giorgio Saluti[c], Andrea Carotti[a], Roccaldo Sardella[a], Antonio Macchiarulo[a], Emidio Camaioni[a,*], Paride Liscio[b]

[a] Department of Pharmaceutical Sciences, University of Perugia, via del Liceo 1, 06123 Perugia, Italy
[b] TES Pharma, via P. Togliatti 22bis, 06073 Terrioli, Corciano, Italy
[c] Istituto Zooprofilattico Sperimentale dell'Umbria e delle Marche, via G. Salvemini, 1, 06126 Perugia, Italy

ARTICLE INFO

Keywords:
Carboxylic acid isosteres, pKa determination
Molecular modeling studies
Diversity-oriented synthesis, fragment based drug design

ABSTRACT

The medicinal chemist toolbox is plenty of (bio)isosteres when looking for a carboxylic acid replacement. However, systematic assessment of acid surrogates is often time consuming and expensive, while prediction of both physicochemical properties (logP and logD) as well as acidity would be desirable at early discovery stages for a better analog design. Herein in this work, to enable decision making on a project, we have synthesized by employing a Diversity-Oriented Synthetic (DOS) methodology, a small library of molecular fragments endowed with acidic properties. By combining *in-silico* and experimental methodologies these compounds were chemically characterized and, particularly, with the aim to know their physicochemical properties, the aqueous ionization constants (pKa), partition coefficients logD and logP of each fragment was firstly estimated by using molecular modeling studies and then validated by experimental determinations. A face to face comparison between data and the corresponding carboxylic acid might help medicinal chemists in finding the best replacement to be used. Finally, in the framework of Fragment Based Drug Design (FBDD) the small library of fragments obtained with our approach showed good versatility both in synthetic and physico-chemical properties.

1. Introduction

According to literature data, the carboxylic acid pharmacophore is widely represented among all marketed drugs accounting for a percentage higher than 13% of total New Molecular Entities (NMEs) approved by FDA from 2015 to 2018 with a record of approvals in 2015 (27% of total approved drugs).[1–3] However, the ability of this functional group to make strong polar and ionic interactions within the protein target may often be translated in poor permeability across biological membranes with undesirable metabolic pathways. In this context, prodrug (e.g. ester prodrugs) strategies or carboxylic acid (bio) isosteres were usually taken from the medicinal chemist toolbox to overcome these limitations, on the route towards improved analogs design. Considering both the *plethora* of acid surrogates available to date and as well as the specific properties for a selected bioisostere, a screening panel of different acidic fragments is generally required during the lead optimization phase, slowing down the entire drug discovery process. Consequently, a systematic assessment of the ionization state of a potential replacement as well as of its physicochemical properties (e.g. as partition coefficient, logD) would be desirable in the early stage of drug discovery to enable prioritization during analog design.[4,5] However, the pursuit of an accurate and all-encompassing pKa prediction method is still a key challenge[6,7] especially when charge delocalization occurs in five membered heterocycles.

Relying on small molecular fragments (MW < 300) as versatile templates for hit compound discovery in the Fragment Based Drug Design (FBDD) field,[8] in this work *in silico* and synthetic skills coupled to experimental measurements of pKa and logD gave the readers access to a systematic assessment of a focused library of fragments endowed with acidic properties. To this end, a Diversity-Oriented Synthetic (DOS) approach was applied, starting from common chemical building blocks in order to enable rapid decisions on the potential replacement to be used.

* Corresponding author.
E-mail address: emidio.camaioni@unipg.it (E. Camaioni).
[1] The two authors contributed equally to this work.

https://doi.org/10.1016/j.bmc.2020.115731
Received 6 April 2020; Received in revised form 28 July 2020; Accepted 19 August 2020
Available online 28 August 2020
0968-0896/

2. Results and discussion

2.1. Fragment design and synthesis

With the aim to prepare a library of aromatic carboxylic acid bioisosteres, as reported in Fig. 1, in the early phase of the design, the 3-methylbenzoic acid (**1**) and the homologue 3-methylphenylacetic acid (**2**) were chosen as acidic reference fragments.

The acidic chain stands for the modified moiety to yield the desired bioisosteres, while the methyl substituent in the aromatic portion represents a modifiable group useful for further elaboration of the fragments (linking, elongation, etc).[8] In the next synthetic step, as a fruitful strategy, the DOS methodology was employed starting from a common building block and obtaining through a small number of steps a library of compounds.[9] In our case, starting from the suitable cyano derivative 3-methylbenzonitrile (**3**), the derivatives **7**, **9**, **11**, **13**, **15** and **17** were planned (Fig. 2). Moreover, in order to evaluate the influence on the physicochemical properties of the fragments of a methylene linker between the aromatic ring and the heterocyclic system, also the derivatives **8, 10, 12, 14, 16** and **18** were designed and synthesized but starting from 3-methylphenylacetonitrile (**4**, Fig. 2).

The synthetic approach, as depicted in the scheme 1, started from the two commercially available building blocks **3** and **4**. As first, the *N*-hydroxybenzamidine intermediates **5**[10] and **6**, were synthesized in quantitative yield by reacting **3** and **4** with hydroxylamine hydrochloride in basic aqueous environment. The reaction was so clean that the obtained derivatives **5** and **6** were directly used for the next steps without any further purification after the usual work-up.

In the next step, starting from **5** and **6**, the fragments **7**–**14** were

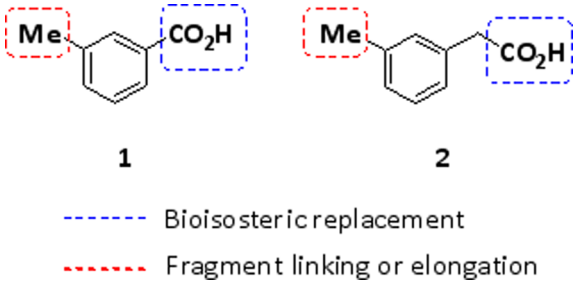

Fig. 1. Reference fragments and work strategy.

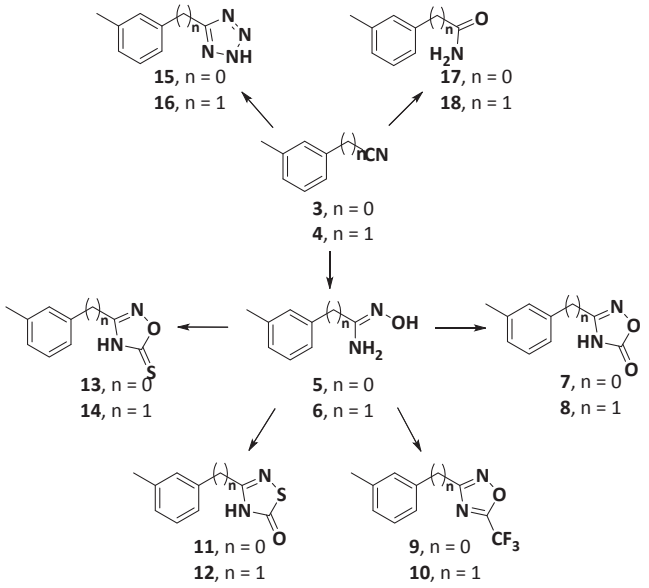

Fig. 2. Fragment based library obtained with a DOS-like synthetic strategy.

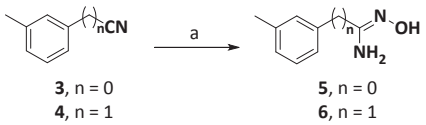

Scheme 1. Synthesis of benzamidine **5** and **6**. Reagent and conditions: (a) H_2O, NH_2OH, $NaHCO_3$, 80 °C, 4 h.

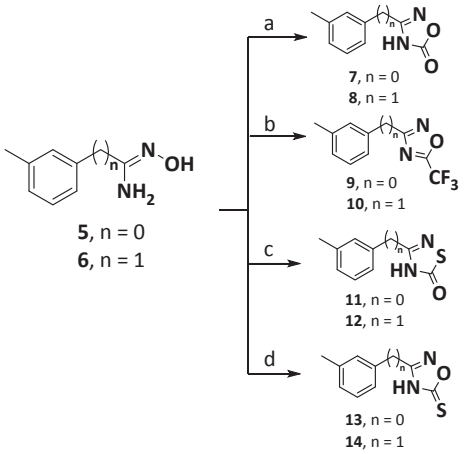

Scheme 2. Synthesis of oxadiazole and thiadiazole derivatives. Reagents and conditions: (a) 1) ethylchloroformate, acetone 0 °C 1 h, then NaOH (5%) 3 h; 2) Pyridine, toluene, reflux 16 h (50–76%); (b) trifluoroacetic anhydride, pyridine, 2 h, 0–25 °C; then HCl 1 N, 0 °C (31–48%); (c) 1) 1,1′-thiocarbonyldiimidazole, THF, r.t., 1 h; 2) $BF_3{\cdot}OEt_2$, THF, r.t., 3 h, (24–71%); (d) 1,1′-thiocarbonyldiimidazole, DBU, dioxane 110 °C, 5 h. (40–83%).

synthesized as reported in the Scheme 2. That is undoubtedly the reason why DOS synthesis shines through many other synthetic methods when it is necessary to build a focused and heterogeneous library from a few precursors. In particular, cyclization of **5** and **6** with ethylchloroformate furnished the oxadiazolones **7**[11] and **8** in 76% and 50% yield respectively. The neutral derivatives **9** and **10**, synthesized to confirm and expand the versatility of our DOS approach, were obtained in good yield (48% and 31% respectively) by cyclization of benzamidine **5** and **6** with trifluoroacetic anhydride. For the synthesis of thiadiazolones **11** and **12**, a known procedure reported in literature was followed.[12] In this case, the cyclization reaction took place in two steps from **5** and **6** with thiocarbonyldiimidazole in the presence of $BF_3(OEt_2)$ afforded the desired compounds **11**[13] and **12** in 71% and 24% yield, respectively.

With a synthetic procedure similar to the one used above for **11** and **12**, the derivatives **13**[14] and **14** were obtained in 83% and 40% yield, respectively.

The two building blocks **3** and **4** were also used for the synthesis of the other fragments **15**–**18** (Scheme 3). Indeed, reaction of the two nitrile derivatives **3** and **4** with sodium azide afforded the corresponding tetrazole derivatives **15**[10,15] and **16**,[16,17] in high yield (85% and 76%, respectively). Interestingly, the amide derivatives **17**[15] and **18**[18] were obtained by using microwave irradiation of **3** and **4,** in basic

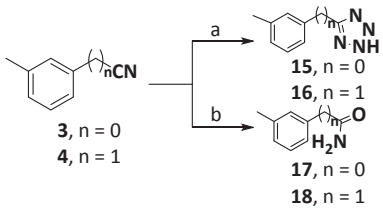

Scheme 3. Synthesis of tetrazoles and amides. Reagent and conditions: (a) sodium azide, Et_3N, toluene, reflux, 16 h (76–85%); (b) potassium carbonate, water, MW, 200 PSI, 130 °C, 30 min (18–50%).

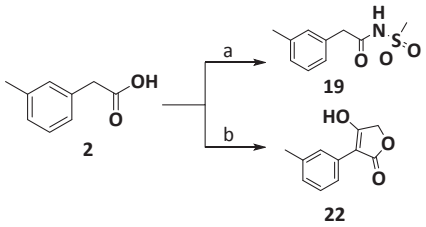

Scheme 4. Synthesis of the derivatives **19** and **22**. Reagents and conditions: (a) CDI, DCM, 30 min; then Et_3N, methanesulfonamide, r.t., 12 h (72%); (b) 1) ethylchloroacetate, THF, Et_3N, reflux, 16 h; 2) sodium *tert*-butoxide, DMF, 0 °C, 1 h, r.t. 5 h (60%).

aqueous medium, in 50% and 18% yield, respectively.

Although our prototypes **1** and **2** could be synthesizable from **3** and **4**, they are commercially available and can be easily exploited for the synthesis of other interesting fragments. An example is reported in Scheme 4.

Indeed, the acidic sulfonamide **19** was obtained in 72% yield by using a coupling reaction between the carboxylic acid **2** and the methanesulfonamide in the presence of CDI. Finally, starting from **2,** the lactone **22** was synthesized. In detail, esterification of **2** with ethylchloroacetate provided the intermediate 2-ethoxy-2-oxoethyl 2-(*m*-tolyl)acetate (**21**) in quantitative yield. Lactonization of the latter in basic conditions provided the desired product **22**,[19] in 60% yield (Scheme 5).

The synthesized fragments were also *in silico* filtered for PAINS (pan-assay interference compounds) activity showing no structural alerts. Furthermore, these fragments are non fluorescent under UV irradiation.

2.2. LogP-LogD/pKa calculations and experimental determinations

These compounds were chemically characterized and, particularly, some of the physico-chemical properties such as their aqueous ionization constants (pKa) and logP/logD were first estimated and then validated by experimental determinations. Beside logP, distribution coefficient (logD) is helpful for the compound characterization during the drug discovery. Conversely to logP, which is referred to the partitioning of the unionized or neutral species between the organic and water layers, logD is concerned to the partitioning of both ionized and unionized species between the two phases at a specific pH values (i.e. at pH 3 and 8). These two parameters describe the same physical property (lipophilicity) but logD accounts for the pH dependence of a molecule in aqueous solution and it is the appropriate descriptor for lipophilicity of ionizable compounds. Thus, physico-chemical properties of each fragment were first estimated *in-silico* by using the software MoKa that implements an algorithm based on descriptors derived from GRID molecular interaction fields, checking also the tautomers.[20] Indeed, many of our studied fragments can behave under different tautomeric rearrangements affecting the results of the cheminformatics tools that estimates physical–chemical properties. To cope with this issue we also employed *ab-initio* calculations. All the molecules were built in all the desired tautomeric states and submitted to a deep conformational analysis. All the conformers were then energetically optimized by the ORCA software[21] (see details in the Experimental section). This procedure allowed us to identify the conformer endowed with the minimum energy (global minima) of each tautomer and to retrieve the Δ energy among the different tautomers, as reported in Table 1 (Δ(ΔG), thus indicating the relative stability.

Several methods have been reported for the determination of pKa,[22] and the most common and accurate is still the potentiometric half-titration volumetric technique (using a glass electrode). Indeed, the experimental pKas were then determined by potentiometric titration implemented in the Sirius T3 apparatus that has been reported to be very sensitive and accurate although its working range is limited to a pKa values ranging from 2 up to 12.[23] The octanol–water partition coefficient (logP) was measured through potentiometric titration in an immiscible biphasic system by using the same Sirius T3 apparatus. In particular, multiple titrations were performed in the aqueous phase at different volumes of water and octanol, in order to evaluate the behavior of the analyte in the partitioning equilibrium. Some of the analyzed fragments were not soluble in water at the used concentration so the stock solution was prepared in DMSO (see experimental details).

Our studied fragments cover a portion of the chemical space (Fig. 3) spanning from 132 to 227 of MW, from 2.64 to over 12 of pKa, and from 0.97 to 2.6 of logP values. Considering *m*-toluic acid **1** as the reference compound, in our hands, fragments bearing respectively the oxadiazol-5(4*H*)-thione (**13**, **14**) and the 5*H*-furan-2-one moiety (**22**) work rather below the acidity of the starting acid **1**, showing experimental values of pKa below 4. Examples of fragments with acidity closest to the starting reference **1** are of note *m*-methylphenylacetic acid **2** and the two tetrazole derivatives **15** and **16**. Interesting values of pKa were obtained with oxadiazol-5(4*H*)-ones **7** and **8** which resulted to be near 5 log unit. Furthermore, we found that some of the determined pKa values fall over the working range as predicted in the case of amides **17** and **18**, but also the two hydroxyamidines **5** and **6** show very weak acidic properties (pKa > 12). Furthermore, **5** and **6** can act as bases. Indeed, we found that these two fragments can be protonated in acidic conditions with a pKa of 4.97 ± 0.03 for **5** and 5.27 ± 0.01 for **6**, respectively. We have also observed a significant increasing in the pKa values when a methylene spacer is placed between the acidic

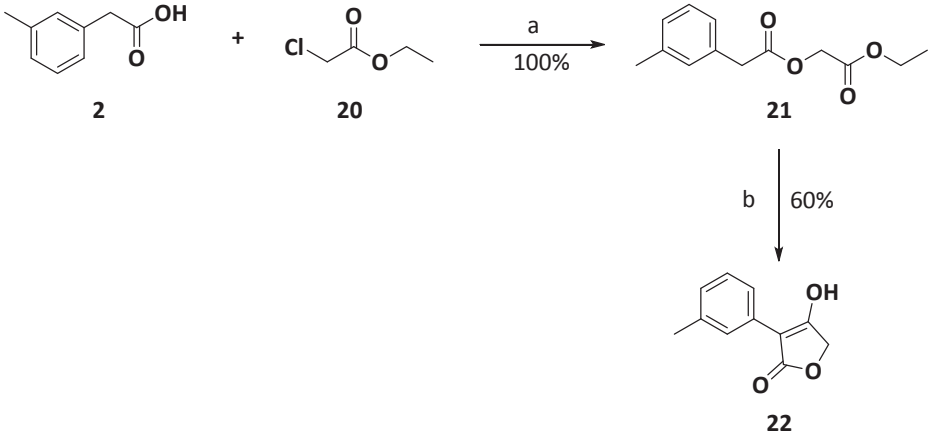

Scheme 5. Synthesis of the derivative **22**. Reagents and conditions: (a) ethylchloroacetate, THF, Et_3N, reflux, 16 h; (b) sodium *tert*-butoxide, DMF, 0 °C, 1 h and then r.t. 5 h.

Table 1
Calculated and experimental properties of test compounds.

#	Structures	MW	Orca Δ(ΔG) Kcal/mol[a]	clogP MoKa	logP SiriusT3	clogD MoKa pH = 3 pH = 8	logD SiriusT3 pH = 3 pH = 8	cpKa Moka[b]	pKa SiriusT3
1	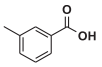	136.1	–	2.3		2.21–1.14	1.40 ± 0.01–0.65 ± 0.02	**3.94** (OH)	3.99 ± 0.03
2	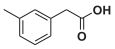	150.1	–	1.8	1.98 ± 0.04	1.80–1.43	1.35 ± 0.01–0.70 ± 0.01	**4.39** (OH)	4.13 ± 0.01
5a	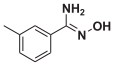	150.2	0.0	2.0	n.d.	−1.80 0.64	n.d.	**12.39** (OH)	> 12
5b	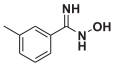		+8.9					9.48 (OH)	
6a	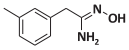	180.2	0.0	2.0	n.d.	−2.18 1.00	n.d.	**12.66** (OH)	> 12
6b	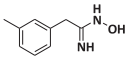		+9.6					9.68 (OH)	
7a	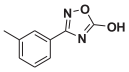	176.2	+14.3	2.5	1.14 ± 0.04	2.50 0.41	0.80 ± 0.01–1.11 ± 0.02	5.90 (OH)	5.12 ± 0.04
7b	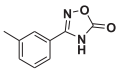		0.0					**7.68** (NH)	
7c	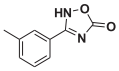		+10.6					–	
8a	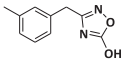	190.2	+15.0	2.6	1.63 ± 0.02	2.30 1.50	1.39 ± 0.01–0.42 ± 0.01	7.27 (OH)	5.59 ± 0.01
8b	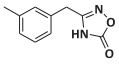		0.0					**8.13** (NH)	
8c	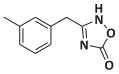		12.3					–	
11a	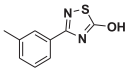	192.2	+12.9	2.6	2.22 ± 0.08	2.60 1.00	2.04 ± 0.02 0.34 ± 0.04	6.41 (OH)	5.99 ± 0.09[c]
11b	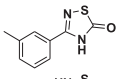		0.0					**9.01** (NH)	
11c	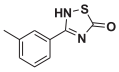		+6.3					–	
12a	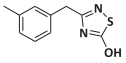	206.3	+13.3	2.4	2.15 ± 0.02	2.39 1.97	2.02 ± 0.01 0.42 ± 0.01	7.78 (OH)	6.35 ± 0.01[c]
12b	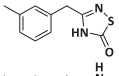		0.0					**9.46** (NH)	
12c	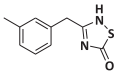		+7.9					–	
13a	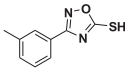	192.2	+8.9	2.7	2.65 ± 0.03	2.66–0.65	1.44 ± 0.01–0.70 ± 0.01	4.14 (SH)	2.64 ± 0.05[c]
13b	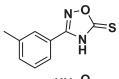		0.0					**6.88** (NH)	
13c	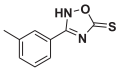		+12.8					–	
14a	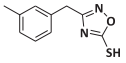	206.3	+9.7	2.5	2.39 ± 0.02	2.47–0.78	1.42 ± 0.01–0.70 ± 0.01	4.36 (SH)	3.19 ± 0.02[c]
14b	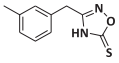		0.0					**7.33** (NH)	
14c	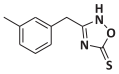		+14.4					–	

(*continued on next page*)

Table 1 (*continued*)

#	Structures	MW	Orca Δ(ΔG) Kcal/mol[a]	clogP MoKa	logP SiriusT3	clogD MoKa pH = 3 pH = 8	logD SiriusT3 pH = 3 pH = 8	cpKa Moka[b]	pKa SiriusT3
15a	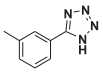	160.2	+2.8	2.3	1.75 ± 0.14	2.25–0.78	1.10 ± 0.01–0.95 ± 0.01	4.32 (NH)	4.07 ± 0.02[c]
15b	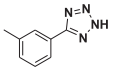		0.0					–	
16a	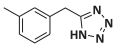	174.2	2.3	2.1	1.51 ± 0.03	2.13 0.55	1.07 ± 0.01–0.96 ± 0.01	5.24 (NH)	4.73 ± 0.03[c]
16b	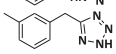		0.0					–	
17	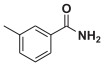	135.2	–	1.2	–	1.20 1.20	n.d.	12.56 (NH_2)	> 12
18	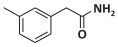	149.2	–	1.1	–	1.05 1.05	n.d.	13.09 (NH_2)	> 12
19	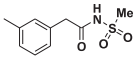	227.3	–	0.9	0.97 ± 0.03	0.87–1.69	0.44 ± 0.11–1.58 ± 0.14	5.40 (NH)	4.63 ± 0.02[c]
22a	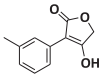	190.2	0.0	1.1	2.32 ± 0.02	−0.88–3.80	1.26 ± 0.02–0.87 ± 0.03	2.56 (OH)	2.95 ± 0.06[c]
22b	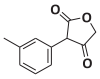		+5.6					3.18 (CH_2)	

[a] Δ(ΔG) in Kcal/mol was estimated at *ab-initio* PBE0/TZVP level of theory and is displayed only for fragments making tautomers.
[b] The putative polarizable functional groups are reported in brackets. The estimated more populated tautomer is highlighted in bold. pKa determinations were performed in water or in.
[c] DMSO (50 mM stock solution). n.d. not determinable, n.i. not ionizable.

functionality and the phenyl ring.

Concerning the lipophilicity, almost all compounds demonstrated experimental logP value comparable to the predicted one. The logP measurement protocol is based on a titration method taking into account the experimental pKas and thus, experimental logP values for compounds **5**, **6**, **17** and **18** were not measured. As a result, all the fragments showed moderate lipophilicity, with the logP values ranging from 0.97 to 2.65, and overall < 3, a value generally accepted as a

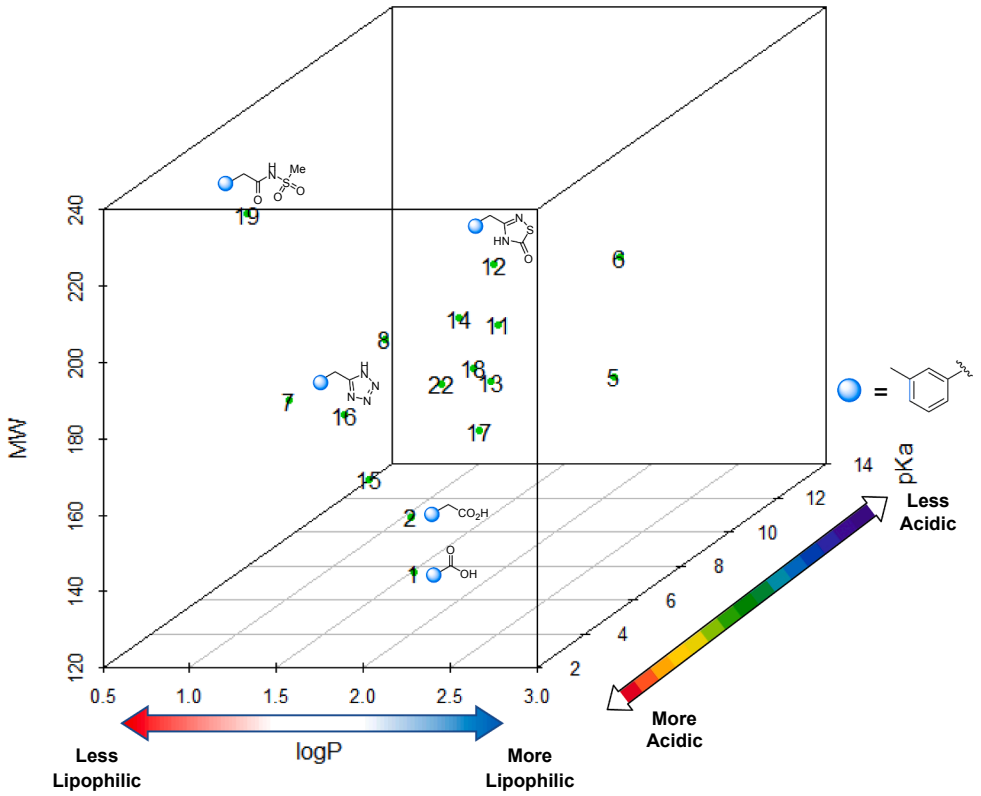

Fig. 3. Chemical space of test fragments represented by size (MW), lipophobicity (logP) and charge in terms of dissociation constant (pKa). For fragments **5**, **6**, **17** and **18** predicted values were plotted.

good cut-off for fragments as starting hits.[24] Regarding the logD values, compound **19** displayed from moderate to good accordance between the *in silico* and the experimental values at both pH (Table 1). Fragments **13** and **14** experimental and predicted logD at pH 8 registered both a value of −0.70. Differently, in the case of free carboxylic acids, the MoKa logD overestimated the pH effect, recording a range between the predictions at pH 8 and 3 higher of 1 unit with respect of the SiriusT3 ones, precisely 3.35 *vs* 2.05 and 3.23 *vs* 2.05 for parent compounds **1** and **2**, respectively. An unsatisfactory prediction performance was also recorded in almost all the rest of the cases. More in general, it should be noted that most of these fragments contains heterocycles that are not usually well parametrized and often needs to be studied by calculations at an *ab-initio* level, thus it was expected to be challenging to predict logD values. Moreover, in the case of prediction systems based on derived empirical models, it is important often the presence of analog compounds in the training set. On the opposite, it must be noted that MoKa achieved a higher performance in the case of pKa estimation, indicating that probably a new model should be trained to obtain more accurate logD predictions.

Derivatives, with a pKa values ranging in close proximity to the neutrality, such as the thiadiazol-5(4H)-ones **11** and **12** could be considered as the best compromises of choice between acidity and lipophilicity when searching for carboxylic acid surrogates or bioisosteres.

The versatility of our fragments could be exploited during the elongation part of the FBDD process. Indeed, the methyl group in *meta* position of the substituted phenyl ring could be modified in the corresponding versatile alkylbromide derivatives by using the classical radical reaction with NBS/AIBN (Fig. 4).

Thus, this approach was validated by some of the authors in a work devoted to the discovery of new inhibitors of the enzyme ACMSD (α-amino-β-carboxymuconate-ε-semialdehyde decarboxylase).[10] For instance, as depicted in Scheme 6, fragment **15** was reacted in AcCN with NBS in the presence of catalytic amount of AIBN to obtain the corresponding tetrazole benzylbromide derivative **23**, in moderate yield. **23** was then coupled with the scaffold 4-oxo-6-thiophen-2-yl-2-thioxo-1,2,3,4-tetrahydropyrimidine-5-carbonitrile (**24**) to obtain the final derivative **25** that was endowed with a very high inhibitory potency (Ki about 0.003 μM) against the targeted enzyme.[10]

The high versatility of benzyl bromide derivatives toward different types of reaction could make this series of acidic fragments a highly desirable building block set for fragment-based drug discovery.

3. Conclusion

The high versatility of the carboxylic acid functional group in drug design lies behind its intrinsic acidity and relies on its ability to establish strong electrostatic interactions and hydrogen-bonds with a target protein thus ensuring also relatively high water solubility to the drug-like molecule. However, the same properties could be also responsible of the “Janus Face” of this versatile functional group, such as low the permeability across biological membranes. From this standpoint, the quest to quickly find additional groups working as acid bio (isosteres) with improved physicochemical properties drove us in this work, with the aim to help medicinal chemists in the choice and in the prioritization of compounds synthesis. Indeed, exploiting a DOS synthetic approach starting from *m*-tolunitrile or *m*-tolylacetonitrile, we reported herein a rapid experimental evaluation of the acidity and lipophilicity of a small series of acidic fragments. Empirical methods such as implemented in MoKa packages possessed fast and predictive capabilities in computational estimation of pKa and logP, while the logD estimation resulted poor. The advanced and automated potentiometric method, Sirius T3, displayed to be very accurate and sensitive in the determination of the pKa, logP and logD values. Finally, fragments obtained with this approach showed good versatility both in synthetic and physico-chemical properties providing low nanomolar ACMSD inhibitor.[10]

In conclusion, when searching for an acid surrogate the medicinal chemist toolbox is plenty of isosteric replacements which might allow a fine tuning, during the drug discovery process, of the physico-chemical properties of the new molecules without loss of potency.

4. Experimentals

4.1. Chemistry

^{1}H NMR spectra were recorded at 200 and 400 MHz and ^{13}C NMR spectra were recorded at 100.6 MHz using the solvents indicated below. Chemical shifts were reported in parts per million (ppm). The abbreviations used are as follows: s, singlet; d, doublet; dd, doublet of doublets; ddd, doublet of doublets of doublets; t, triplet; dt, doublet of triplets; q, quartet; qui, quintet. The final products were purified by flash chromatography on silica gel 60 (0.040–0.063 mm). TLC were performed on aluminum backed silica plates (silica gel 60 F254). All the reaction were performed under nitrogen atmosphere using distilled solvent. All reagents were from commercial sources. The HPLC analytical scale measurements were carried out on a Shimadzu LC Workstation Class LC-10 equipped with SCL-10 A VP system controller, a LC-10AT VP high pressure binary gradient delivery system, an SPD-10˚ VP variable-wavelenght UV–vis detector, and a Rheodyne 7725i injector with a 20 μL stainless steel loop. The chromatographic profile was obtained with EZ Start software. All analytical runs were performed by employing a H_2O/CH_3CN/TFA (60/40/0.1 v/v/v) solution as the mobile phase. HPLC grade water was obtained from a tandem Milli-Ro / Milli-Q apparatus. A Grace Smart C18 250 × 4.6 mm i.d. 5 μm 100 Å analytical column was used after previous conditioning by passing through the column the selected mobile phase for at least 45 min. The UV detection wavelengths were set at 254 and 210 nm. Samples for analytical-scale analyses were prepared in approximate concentration between 0.1 and 0.5 mg/mL in filtered mobile phase components with auxiliary DMSO, if necessary, and sonicated until completely dissolved. The GC–MS analyses were performed on an Agilent 7890A GC coupled to a triple quadrupole mass spectrometer Agilent 7000 MS system (Agilent Technologies, Waldbronn, Germany). 1 μL of the powder solubilized in ethylacetate was injected in a programmable temperature vaporization (PTV) inlet. The chromatographic separation was achieved using a Restek Rtx®-5MS column (Bellefonte, PA) (30 m × 0.25 mm × 0.25 μm) as follows: 2 min hold at 70 °C, ramp to 300 °C at 10 °C min^{-1}, 3 min hold at 300 °C. The mass spectrometric acquisition was performed in Full Scan mode (*m/z* 50–230).

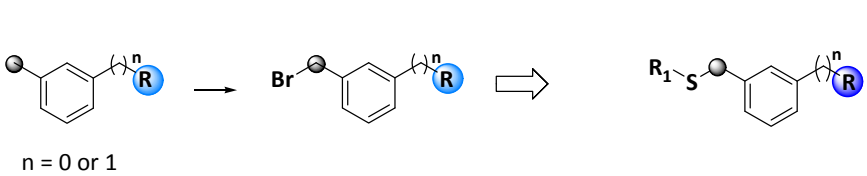

Fig. 4. General approach of FBDD with our synthesized fragments.

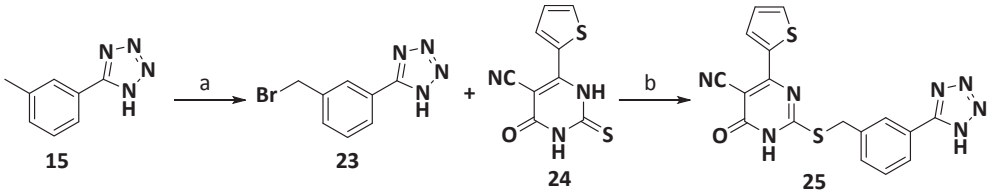

Scheme 6. Synthesis of the 1,6-dihydro-6-oxo-2-[[[3-(2H-tetrazol-5yl)phenyl]methyl]thio]-(2-thienyl)-5-pyrimidinecarbonitrile. Reagents and conditions: (a) NBS, AIBN, AcCN, reflux, 16 h. (b) DIPEA, DMSO, rt, 16 h.

4.2. General procedure A

To an aqueous solution (7 mL) of hydroxylamine hydrochloride (1.42 g, 20.5 mmol) and sodium bicarbonate (1.72 g, 20.5 mmol), a solution the appropriate nitrile derivative (2 mL, 17 mmol) in ethanol (13 mL) was slowly added dropwise. The reaction mixture was heated to reflux (80 °C) for 4 h. When the reaction was ended the solvent was removed under reduced pressure and the crude was poured into water and extracted with ethyl acetate (3 × 30 mL). The combined organic layers were washed with saturated aqueous sodium chloride and dried over Na_2SO_4 then concentrated under reduced pressure.

4.3. N-hydroxy-3-methyl-benzamidine (5)

Starting from 3-methylbenzonitrile (2 mL, 17 mmol) and following the general procedure A the title compound was obtained as a thick oil which gradually turned into a white crystalline solid (2.5 g, quantitative yield). m.p.: 86–89 °C

^{1}H NMR (400 MHz, DMSO-d_6) δ 2.31 (s, 3H), 5.75 (s, 2H), 7.16–7.26 (m, 2H), 7.44–7.48 (m, 2H), 9.6 (s, 1H).

^{13}C NMR (100.6 MHz, DMSO-d_6): δ 21.48, 122.97, 126.39, 128.39, 129.87, 133.70, 137.55, 151.28.

GC–MS: RT 7.2 min; *m/z* 117.0 ($[M-NH_2OH]^+$, 100), 116.0 (65).

HPLC: RT = 3.04 min (> 96%)

Analytical data are in accordance with those reported elsewhere.[10]

4.4. N-Hydroxy-2-(3-methylphenyl)-acetamidine (6)

Starting from 2-(3-methylphenyl)acetonitrile (0.6 mL, 4.57 mmol) and following the general procedure A the title compound was obtained as a yellow oil (688 mg, quantitative yield).

^{1}H NMR (400 MHz, DMSO-d_6) δ 2.31 (s, 3H), 3.20 (s, 2H), 5.36 (s, 2H), 7.-7.18 (m, 4H), 8.87 (s, 1H).

^{13}C NMR (100.6 MHz, DMSO-d_6) δ 21.41, 37.52, 126.19, 127.23, 128.39, 129.71, 137.45, 138.26, 152.36.

GC–MS: RT 9.3 min; *m/z* 131.0 ($M-NH_2OH]^+$, 100), 116.0 (90), 104.0 (76).

HPLC: RT = 3.27 min (> 95%).

4.5. General procedure B

To a solution of the appropriate nitrile derivative (1 g, 8.53 mmol) in toluene (15 mL) NaN_3 (564 mg, 9,4 mmol) and Et_3N HCl (1.86 g, 9.4 mmol) were added. The mixture was refluxed for 16 h. Then the reaction was quenched with a mixture of ice/water and stirred for 30 min. The organic phase was separated from aqueous one and the latter was acidified with HCl 1 N and extracted with EtOAc (3 × 15 mL). The combined organic layers were washed with NaCl saturated aqueous solution and dried over sodium sulfate and concentrated under vacuum. The title compound was crystallized from Et_2O.

4.6. 5-m-Tolyl-1H-tetrazole (15)

Starting from 3-methylbenzonitrile (**3**, 1.0 g, 8.53 mmol) and following the general procedure B the desired product **15** was obtained as a white crystalline solid (1.0 g, yield 85%). m.p.: 145–147 °C.

^{1}H NMR (400 MHz, DMSO-d_6) δ 2.40 (s, 3H), 7.39 (d, J = 7.5 Hz, 1H), 7.48 (t, J = 7.6 Hz, 1H), 7.83 (d, J = 7.7 Hz, 1H), 7.8 (s, 1H). ^{13}C NMR (100.6 MHz, DMSO-d_6): δ 21.3, 124.4, 127.7, 129.7, 132.2, 139.2, 155.7.

GC–MS: RT 16.3 min; *m/z* 132.0 (100), 117.0 (68), 116.0 (50), 104.1 (34), 160.1 ($M^{+\cdot}$, 15)

HPLC: RT = 5.43 min (> 98%)

Analytical data are in accordance with those reported in literature.[10,15]

4.7. 5-[(3-Methylphenyl)methyl]-1H-tetrazole (16)

Starting from 2-(3-methylphenyl)acetonitrile (**4**, 2 mL, 15.25 mmol) and following the general procedure F the title compound was obtained as a white solid (2.05 g, yield 76%). m.p.: 132–136 °C.

^{1}H NMR (400 MHz, DMSO-d_6) δ 2.26 (s, 3H), 7.04–7.08 (m, 2H), 7.31 (t, 1H, J = 7.51 Hz)

^{13}C NMR (100.6 MHz, DMSO-d_6) δ 21.33, 126.10, 128.04, 129.03, 129.64, 136.20, 138.29.

GC–MS: RT 16.9 min; *m/z* 105.0 (100), 131.0 (23), 174.1 (M^+, 18), 116.0 (17).

HPLC: RT = 5.59 min (> 98%).

Analytical data are in accordance with those reported in literature.[16,17]

4.8. General procedure C

In a microwave sealed tube, the appropriate nitrile derivative (1.54 mL, 12.8 mmol) and potassium carbonate (707 mg, 5.12 mmol) were suspended in water (10 mL). The mixture was irradiated at 130 °C at 200 PSI and 200 W for 30 min. The crystalline solid obtained was collected by filtration. The water phase was extracted with EtOAc (3 × 20 mL) and the combined organic layers were washed with NaCl saturated aqueous solution and dried over Na_2SO_4. The solvent was evaporated under reduced pressure affording the desired product combined with the crystalline solid isolated by filtration.

4.9. 3-Methylbenzamide (17)

Starting from **3** (1.54 mL, 12.8 mmol) and following the general procedure C the desired product **17** was obtained as opalescent crystals (870 mg, Yield 50%). m.p.: 92–94 °C

^{1}H NMR (400 MHz, DMSO-d_6) δ 2.34 (s, 3H), 7.31–7,33 (m, 3H), 7.64 (s, 1H), 7.69 (s, 1H), 7.91 (s, 1H)

^{13}C NMR (100.6 MHz, DMSO-d_6) δ 21.36, 124.98, 128.49 (2C), 132.17, 134.62, 137.83, 168.41.

GC–MS: RT 12.0 min; *m/z* 119.0 (100), 135.1 ($M^{+\cdot}$, 65)

HPLC: RT = 4.23 min (> 98%)

Analytical data are in accordance with the literature ones.[15]

4.10. 3-Methylphenylacetamide (18)

Starting from 2-(3-methylphenyl)acetonitrile (**4**, 0.3 mL, 2.3 mmol) and following the general procedure C the desired compound **18** was obtained as an opalescent crystalline solid (60 mg, yield 18%). m.p.: 146–148 °C.

^{1}H NMR (400 MHz, DMSO-d_6) δ 2.27 (s, 3H), 3.34 (s, 2H), 6.85 (s,

1H), 7.03–7.06 (m, 2H), 7.16 (s, 1H), 7.43 (s, 1H).

^{13}C NMR (100.6 MHz, DMSO-d_6) δ 21.39, 42.63, 126.53, 127.29, 128.46, 130.10, 136.77, 137.53, 172.68.

GC–MS: RT 12.6 min; *m/z* 106.1 (100), 149.1 ($M^{+\cdot}$, 38).

HPLC: RT = 4.53 min (> 98%)

Analytical data are in accordance with literature ones.[18]

4.11. General procedure D

To a solution of amidine (2.5 g, 17 mmol) in dry acetone (10 mL) ethylchloroformate (1,8 mL, 18.72 mmol) solution in acetone (10 mL) was added dropwise at 0 °C. The reaction was stirred for 1 h under these conditions. Then an aqueous solution of sodium hydroxide (5%, 15 mL) was added at room temperature and the mixture was stirred for additional 3 h. The formation of a white precipitate was observed. Then the solvent was removed under reduced pressure and the crude was partitioned between water and ethylacetate (3 × 30 mL). The combined organic layers were washed with saturated solution of NaCl and dried over Na_2SO_4 then concentrated under vacuum. The product was purified by flash chromatography eluting with PET/EtOAc (from 0 to 40% of EtOAc) affording the intermediate as a white solid (3.58 g, 16.12 mmol). The latter was solubilized in toluene (90 mL) and pyridine (13.03 mL, 161.12 mmol) was added dropwise to the mixture. The reaction mixture was heated to reflux (110 °C) and stirred at this temperature for 16 h. Then the mixture was diluted with HCl 1 N (100 mL) and extracted with EtOAc (3 × 40 mL). The combined organic layers were washed with saturated solution of NaCl and dried over Na_2SO_4 then concentrated under vacuum. The crude was purified by flash chromatography eluting with PET/EtOAc (from 0% to 40% of EtOAc) affording the desired product.

4.12. 3-(3-methylphenyl)-4,5-dihydro-1,2,4-oxadiazol-5-one (7)

Starting from **5** (2.5 g, 17 mmol) and following the general procedure D the desired product **7** was obtained as a white solid (2.3 g, yield 76%). m.p.: 138–140 °C

^{1}H NMR (400 MHz, DMSO-d_6) δ 2.38 (s, 3H), 7.41–7.49 (m, 2H), 7.59–7.69 (m, 2H), 12.93 (bs, 1H).

^{13}C NMR (100.6 MHz, DMSO-d_6) δ 21.25, 123.65, 126.77, 129.60, 133.26, 139.18, 157.82, 160.37.

GC–MS: RT 17.8 min; *m/z* 117.0 (100), 116.0 (65), 133.0 (26), 176.1 ($M^{+\cdot}$, 18).

HPLC: RT = 7.00 min (> 98%)

Analytical data are in accordance with literature ones.[11]

4.13. 3-[(3-methylphenyl)methyl]–2H-1,2,4-oxadiazol-5-one (8)

Starting from **6** (688 mg, 4.19 mmol) and following the general procedure D the desired product **8** was obtained as a yellowish solid (485 mg yield 50%). m.p.: 106–109 °C

^{1}H NMR (400 MHz, DMSO-d_6) δ 2.29 (s, 3H), 3.82 (s, 2H), 7.07–7.12 (m, 3H), 7.24 (t, 1H, J = 7.4 Hz), 12.30 (bs, 1H).

^{13}C NMR (100.6 MHz, DMSO-d_6) δ 21.31, 30.96, 126.28, 128.37, 129.04, 129.82, 134.08, 138.34, 159.45, 160.23.

GC–MS: RT 17.8 min; *m/z* 131.0 (100), 116.0 (76), 104.0 (70), 190.1 ($M^{+\cdot}$, 12).

HPLC: RT = 7.12 min (> 95%).

4.14. General procedure E

To a solution of the amidine (600 mg, 4 mmol) in dioxane (20 mL) treated 1–1-thiocarbonyldiimidazole (1.07 g, 6 mmol) was added followed by 1,5-diazabicyclo(5.4.0)undec-5-ene (DBU, 2.42 mL, 16 mmol). The resulting mixture was heated at 110 °C for 5 h. Then the solvent was evaporated under vacuum and the crude was diluted with DCM (50 mL) and washed with HCl 1 N (3 × 60 mL). The organic solvent was removed under reduced pressure and the crude was purified by flash chromatography eluting with DCM/MeOH (from 0% to 1% of MeOH).

4.15. 3-(3-Methylphenyl)-4,5-dihydro-1,2,4-oxadiazol-5-thione (13)

Starting from the *N*-Hydroxybenzamidine (**5**, 600 mg, 4 mmol) and following the general procedure E the desired compound **13** was obtained as a yellow solid (640 mg, yield 83%) m.p.: 153.6–159.2 °C

^{1}H NMR (400 MHz, DMSO-d_6) δ 2.39 (s, 3H), 7.39–7.6 (m, 4H), 14.45 (bs, 1H).

^{13}C NMR (100.6 MHz, DMSO-d_6) δ 21.24, 122.07, 124.43, 127.59, 129.71, 133.68, 139.33, 159.44, 187.81.

GC–MS: RT 18.0 min; *m/z* 117.0 (100), 149.0 (90), 116.0 (65), 192.0 ($M^{+\cdot}$, 53).

HPLC: RT = 11.93 min (> 98%)

Other analytical data are known in literature.[14]

4.16. 3-[(3-Methylphenyl)methyl]-4,5-dihydro-1,2,4-oxadiazol-5-thione (14)

Starting from **6** (400 mg, 2.44 mmol) and following the general procedure E the desired product **14** was obtained as a brown solid (200 mg, yield 40%). m.p: 85–90 °C.

^{1}H NMR (400 MHz, DMSO-d_6) δ 2.29 (s, 3H), 3.96 (s, 2H), 7.12–7.08 (m, 2H), 7.26 (s, 1H), 14.35 (bs, 1H)

^{13}C NMR (100.6 MHz, DMSO-d_6) δ 21.32, 29.70, 126.42, 128.47, 129.06, 129.96, 133.91, 138.36, 161.12, 187.40.

GC–MS: RT 18.0 min; *m/z* 105.0 (100), 206.1 ($M^{+\cdot}$, 85), 131.0 (80), 116.0 (75).

HPLC: RT = 12.25 min (> 98%).

4.17. General procedure F

To a solution of the appropriate amidine (1.0 g, 6.7 mmol) in dry THF (10 mL) 1,1-thiocarbonyldiimidazole (1.8 g, 10.1 mmol) was added. The reaction was stirred at room temperature for 1 h. The mixture was poured into water and extracted with DCM (3 × 30 mL). The combined organic layers were washed with saturated solution of NaCl and dried over Na_2SO_4 and concentrated under reduced pressure. Then the crude was dissolved in dry THF (15 mL) and of boron trifluoride diethyl etherate 46,5% solution (6.14 mL, 20.1 mmol) was added dropwise to the mixture. The reaction was stirred at room temperature for 3 h and an orange precipitate was observed. The mixture was then diluted with water and extracted with EtOAc (3 × 30 mL), washed with saturated solution of NaCl and dried over Na_2SO_4. The crude was purified by flash chromatography eluting with PET/EtOAc (from 0% to 15% of EtOAc).

4.18. 3-(3-Methylphenyl)-1,2,4-thiadiazol-5-one (11)

Starting from **5** (1.0 g, 6.7 mmol) and following the general procedure F the desired product **11** was obtained as a white solid (918 mg, yield 71%). m.p.: 168–172 °C.

^{1}H NMR (400 MHz, DMSO-d_6) δ 2.36 (s, 3H), 7.36–7.43 (m, 2H), 7.71–7.78 (m, 2H), 13.36 (bs, 1H)

^{13}C NMR (100.6 MHz, DMSO-d_6) δ 21.31, 124.07, 127.35, 128.83, 129.26, 132.42, 138.76, 155.17, 179.94.

GC–MS: RT 18.1 min; *m/z* 149.0 (100), 117.0 (70), 116.0 (55), 192.0 ($M^{+\cdot}$, 53).

HPLC: RT = 9.16 min (> 98%).

Analytical data are in accordance with literature ones.[13]

4.19. 3-[(3-Methylphenyl)methyl]-1,2,4-thiadiazol-5-one (12)

Starting from **6** (1.0 g, 6.1 mmol) and following the general

procedure F the desired compound **12** was obtained as a white solid (300 mg, Yield 24%). m.p.: 112–114 °C. ^{1}H NMR (400 MHz, DMSO-d_6) δ 2.28 (s, 3H), 3.8 (s, 2H), 7.05–7.09 (m, 3H), 7.2 (s, 1H), 12.86 (bs, 1H).

^{13}C NMR (100.6 MHz, DMSO-d_6) δ 21.36, 37.14, 126.33, 128.07, 128.90, 129.88, 135.31, 138.13, 157.81, 179.71.

GC–MS: RT 16.9 min; *m/z* 105.0 (100), 131.0 (23), 174.1 ($M^{+\cdot}$, 18), 116.0 (17).

HPLC: RT = 8.07 min (> 98%).

4.20. 2-(3-methylphenyl)-N-methylsulfonylacetamide (19)

To a solution of *m*-tolyl acetic acid (500 mg, 3.33 mmol) in DCM (15 mL), 1-carbonyldiimidazole (CDI, 589 mg, 3.63 mmol) was added. The resulting solution was stirred at room temperature for 30 min. After this time Et_3N (0.93 mL, 6.66 mmol) and methylsulfonamide (634 mg, 6.66 mmol) were added to the mixture and stirring was continued at room temperature for 12 h. The reaction was cooled to 0 °C then $KHPO_4$ buffer solution (50 mL, pH = 2.4) was added. The aqueous layer was separated and extracted with EtOAc (3 × 25 mL). The combined organic layers were washed with brine and dried over Na_2SO_4 and concentrated under vacuum. The title compound was obtained as a colourless oil which crystallized slowly into a white solid (549 mg, yield 72%). m.p. = 105.3–108.2 °C. ^{1}H NMR (400 MHz, DMSO-d_6) δ 2.28 (s, 3H), 3.09 (s, 3H), 3.47 (s, 2H), 7.03–7.05 (m, 3H), 7.19 (t, J = 7.49 Hz, 1H).

^{13}C NMR (100.6 MHz, DMSO-d_6) δ 9.15, 21.38, 40.50, 41.11, 43.54, 46.10, 126.79, 127.58, 128.52, 130.38, 135.48, 137.62, 172.30.

GC–MS: RT 17.1; *m/z* 105.0 (100), 132.0 (95), 227.1 ($M^{+\cdot}$, 17).

HPLC: RT = 6.47 min (> 96%).

4.21. 4-Hydroxy-3-m-tolyl-5H-furan-2-one (22)

To a solution of *m*-toluic acid (2 g, 13.3 mmol) and ethylchloroacetate (2.14 mL, 19.9 mmol) in THF (10 mL) was added Et_3N (2.8 mL, 19.9 mL). Stirring was continued at reflux for 16 h. A white solid was formed. The solid was filtered through a sintered pad. The filter cake was washed with THF (3 × 5 mL). The solvent was removed under reduced pressure. The intermediate 2-ethoxy-2-oxoethyl 2-(*m*-tolyl)acetate was obtained as a yellow oil quantitative yield and used directly for the next step (3.7 g). To solution of the starting intermediate (3.7 g, 15.6 mmol) in DMF (15 mL) sodium *tert*-butoxide (3.5 g, 31.3 mmol) was added portionwise. Stirring was continued at 0 °C for 1 h and for additional 5 h at room temperature. The mixture was diluted with water, extracted with EtOAc (3 × 20 mL). the combined organic layers were washed with NaCl saturated aqueous solution and dried over Na_2SO_4 and concentrated under vacuum. 800 mg The desired compound **24** was obtained as a white solid after shredding with Et_2O (800 mg, yield 30%). m.p.: 208–210 °C.

^{1}H NMR (400 MHz, DMSO-d_6): δ 2.39 (s, 3H, CH_3); 4.88 (s, 2H, CH_2); 7.42–7.46 (m, 1H, ArH); 7.72–7.85 (m, 3H, ArH); 12.58 (s, 1H, OH).

^{13}C NMR (100.6 MHz, DMSO-d_6) δ 21.68, 66.40, 97.75, 123.94, 127.22, 127.43, 128.38, 130.83, 137.36, 173.37, 175.35.

GC–MS: RT 16.9; *m/z* 190.1 ($M^{+\cdot}$, 100), 132.0 (75), 103.0 (68), 117.0 (42), 161.0 (38).

HPLC: t_R = 7.15 min (> 98%).

Analytical data are in accordance with those reported by Wang et al.[19]

4.22. LogPs and pKas determination

Experimental pKa values were determined by means of a SiriusT3 instrument (Sirius Analytical Instruments Ltd., Forest Row, E. Sussex, UK). Analyzed compounds were dissolved in water or in DMSO preparing stock solutions with a concentration of 50 mM. Details of the experimental method were reported elsewhere.[25] SiriusT3 instrument works in a pH range from 2 to 12 and the protocol employed takes into account only the compounds with pK_a value into the range. The octanol–water partition coefficient (logP) was measured through potentiometric titration in an immiscible biphasic system using a SiriusT3 apparatus. Thus, potentiometric logPs (pH-metric medium logP) were recordered at 25 °C in a constant ionic strength (0.15 M KCl). This analysis required the pKa values determined in the previous analysis using the same instrument. LogD values are also related to logP taking into account the pKa of each compound and the pH values were fixed at 3 and 8. SiriusT3 allowed us to determine experimentally logP and pKa for all the compounds when the pKa value is included in the pKa working range of 2–12. Applying the following equation,

$$logD_{(pH)} = logP - log\left[1 + 10^{(pH-pK_a)}\right]$$

logD values were determined for each acidic fragments focusing the pH values to 3 and 8.

The compounds were collected in stock solutions 50 mM in DMSO solvent, and for each sample the analysis has been carried out using 150 μL of stock solution.

5. Computational methods

The molecules were built in all the tautomeric states of interest, using the Maestro (version 12, Schrödinger, LLC, New York, NY, 2019) interface present in the Schrödinger Suite 2019-2. Next, a conformational search was performed with MacroModel (version 12.4, Schrödinger, LLC, New York, NY, 2019) and the geometries of each conformer energetically optimized with ORCA 4.1.2 software,[21] leading to the identification of the global minimum. In particular, the conformational analysis was performed using the OPLS3e force field and the "Mixed torsional/Low-mode sampling", executing 1000 steps, retaining per each molecule all the conformers lying in a window of 10.0 kcal mol^{-1} from the global minimum and using water as the solvent. The torsional sampling involves multiple Monte Carlo minimum searches for global exploration, and the low mode conformational search allows for automatic local exploration. The conformers were considered to be different if the maximum atom deviation for any pair of corresponding atoms exceeds the threshold of 0.5 Å. All the options were set as default with the exception of the "Torsional sampling options" that were changed from "Intermediate" to "Extended" in order to improve the conformational space searched. This step produced a total of 333 conformers that were all submitted to a quantum mechanical energy optimization by using the PBE0 functional[26] that was used in combination with the TZVP basis set[27] and the conductor-like polarizable continuum model (CPCM keyword)[28] to keep in consideration the water environment. Finally the level of accuracy was set to *tightscf*. The resulting conformer of each tautomeric state was used to identify the global minimum of each compound. This value was then used to compute the energy difference (ΔΔG) among different tautomeric states of the same molecule, thus allowing to identify the preferred state(s) of that species in water.

The global minima conformers were used as input for the MoKa v3.1.1 software[20] to estimate the pKa and the logP/logD values. Similarly, the same input was used in the Canvas program (Schrödinger Release 2019–2: Canvas, version 4.0, Schrödinger, LLC, New York, NY (USA)) to check for PAINS compounds by applying the relative filter.[29]

6. Notes

All co-authors have agreed with the submission of the final manuscript and participated in the research.

Funding

University of Perugia (Fondo Ricerca di Base 2018) is gratefully acknowledged for the financial support.

Declaration of Competing Interest

The authors declare that they have no known competing financial interests or personal relationships that could have appeared to influence the work reported in this paper.

References

[1]. Flick AC, Ding HX, Leverett CA, et al. Synthetic approaches to the new drugs approved during 2015. *J Med Chem.* 2017;60:6480–6515. https://doi.org/10.1021/acs.jmedchem.7b00010.

[2]. Flick AC, Leverett CA, Ding HX, et al. Synthetic approaches to the new drugs approved during 2017. *J Med Chem.* 2019;62:7340–7382. https://doi.org/10.1021/acs.jmedchem.9b00196.

[3]. Flick AC, Leverett CA, Ding HX, et al. Synthetic approaches to new drugs approved during 2018. J Med Chem. 2020; in press. 10.1021/acs.jmedchem.0c00345.

[4]. Milletti F, Storchi L, Goracci L, et al. Extending pKa prediction accuracy: high-throughput pKa measurements to understand pKa modulation of new chemical series. *Eur J Med Chem.* 2010;45:4270–4279. https://doi.org/10.1016/j.ejmech.2010.06.026.

[5]. Manallack DT. The pK(a) distribution of drugs: Application to drug discovery. *Perspect Medicin Chem.* 2007;1:25–38. https://doi.org/10.1177/1177391X0700100003.

[6]. Caine BA, Dardonville C, Popelier PLA. Prediction of aqueous pK (a) Values for guanidine-containing compounds using ab initio gas-phase equilibrium bond lengths. *ACS Omega.* 2018;3:3835–3850. https://doi.org/10.1021/acsomega.8b00142.

[7]. Jensen JH, Swain CJ, Olsen L. Prediction of pK(a) values for druglike molecules using semiempirical quantum chemical methods. *J Phys Chem A.* 2017;121:699–707. https://doi.org/10.1021/acs.jpca.6b10990.

[8]. Sheng C, Zhang W. Fragment informatics and computational fragment-based drug design: an overview and update. *Med Res Rev.* 2013;33:554–598. https://doi.org/10.1002/med.21255.

[9]. Collins I, Jones AM. Diversity-oriented synthetic strategies applied to cancer chemical biology and drug discovery. *Molecules.* 2014;19:17221–17255. https://doi.org/10.3390/molecules191117221.

[10]. Pellicciari R, Liscio P, Giacchè N, et al. α-Amino-β-carboxymuconate-ε-semialdehyde decarboxylase (ACMSD) inhibitors as novel modulators of de novo nicotinamide adenine dinucleotide (NAD+) biosynthesis. *J Med Chem.* 2018;61:745–759. https://doi.org/10.1021/acs.jmedchem.7b01254.

[11]. Yu X, Chen K, Yang F, Zha S, Zhu J. Oxadiazolone-enabled synthesis of primary azaaromatic amines. *Org Lett.* 2016;18:5412–5415. https://doi.org/10.1021/acs.orglett.6b02814.

[12]. Lassalas P, Gay B, Lasfargeas C, et al. Structure property relationships of carboxylic acid isosteres. *J Med Chem.* 2016;59:3183–3203. https://doi.org/10.1021/acs.jmedchem.5b01963.

[13]. Kohara Y, Kubo K, Imamiya E, Naka T. A facile synthesis of 3-substituted 5-oxo-1,2,4-thiadiazoles from amidoximes. *J Heterocycl Chem.* 2000;37:1419–1423. https://doi.org/10.1002/jhet.5570370603.

[14]. Sonawane AD, Rode ND, Nawale L, et al. Synthesis and biological evaluation of 1,2,4-triazole-3-thione and 1,3,4-oxadiazole-2-thione as antimycobacterial agents. *Chem Biol Drug Des.* 2017;90:200–209. https://doi.org/10.1111/cbdd.12939.

[15]. Maiti Bag S, Jayarajan R, Dutta U, Chowdhury R, Mondal R, Maiti D. Remote meta-C-H cyanation of arenes enabled by a pyrimidine-based auxiliary. *Angew Chem Int Ed Engl.* 2017;56:12538–12542. https://doi.org/10.1002/anie.201706360.

[16]. Satyanand K, Shristy D, Nisha S, Kumar AS. $(NH_4)_2Ce(NO_3)_6$ as an inexpensive, eco-friendly, efficient catalyst for the synthesis of 5-substituted 1-*H* tetrazoles from nitriles. *Tetrahedron Lett.* 2014;55:6034–6038. https://doi.org/10.1016/j.tetlet.2014.09.010.

[17]. Liao AM, Wang T, Cai B, et al. Design, synthesis and evaluation of 5-substituted 1-H-tetrazoles as potent anticonvulsant agents. *Arch Pharm Res.* 2017;40:435–443. https://doi.org/10.1007/s12272-016-0881-y.

[18]. Jaiswal Y, Kumar Y, Thakur R, Pal J, Subramanian R, Kumar A. Primary amide directed regioselective ortho-C-H-arylation of (aryl)acetamides. *J Org Chem.* 2016;81:12499–12505. https://doi.org/10.1021/acs.joc.6b02353.

[19]. Wang XD, Wei W, Wang PF, et al. Synthesis, molecular docking and biological evaluation of 3-arylfuran-2(5H)-ones as anti-gastric ulcer agent. *Bioorg Med Chem.* 2015;23:4860–4865. https://doi.org/10.1016/j.bmc.2015.05.026.

[20]. Milletti F, Storchi L, Sforna G, Cruciani G. New and original pKa prediction method using grid molecular interaction fields. *J Chem Inf Model.* 2007;47:2172–2181. https://doi.org/10.1021/ci700018y.

[21]. Neese F. The ORCA program system. *WIREs Comput Mol Sci.* 2012;2:73–78. https://doi.org/10.1002/wcms.1327.

[22]. Reijenga J, van Hoof A, van Loon A, Teunissen B. Development of methods for the determination of pKa values. *Anal Chem Insights.* 2013;8:53–71. https://doi.org/10.4137/ACI.S12304.

[23]. Box K, Bevan C, Comer J, Hill A, Allen R, Reynolds D. High-throughput measurement of pKa values in a mixed-buffer linear pH gradient system. *Anal Chem.* 2003;75:883–892. https://doi.org/10.1021/ac020329y.

[24]. Hajduk PJ. Fragment-based drug design: how big is too big? *J Med Chem.* 2006;49:6972–16876. https://doi.org/10.1021/jm060511h.

[25]. Coletti A, Camponeschi F, Albini E, et al. Fragment-based approach to identify IDO1 inhibitor building blocks. *Eur J Med Chem.* 2017;141:169–177. https://doi.org/10.1016/j.ejmech.2017.09.044.

[26]. Perdew JP, Burke K, Ernzerhof M. Generalized gradient approximation made simple. *Phys Rev Lett.* 1996;77:3865–3868. https://doi.org/10.1103/PhysRevLett.77.3865.

[27]. Weigend F, Ahlrichs R. Balanced basis sets of split valence, triple zeta valence and quadruple zeta valence quality for H to Rn: Design and assessment of accuracy. *Phys Chem Chem Phys.* 2005;7:3297–3305. https://doi.org/10.1039/B508541A.

[28]. Barone V, Improta R, Rega N. Computation of protein pK's values by an integrated density functional theory/Polarizable Continuum Model approach. *Theor Chem Acc.* 2004;111:237–245. https://doi.org/10.1007/s00214-003-0541-4.

[29]. Baell JB, Holloway GA. New substructure filters for removal of pan assay interference compounds (PAINS) from screening libraries and for their exclusion in bioassays. *J Med Chem.* 2010;53:2719–2740. https://doi.org/10.1021/jm901137j.